Regular Article

PHYSICAL CHEMISTRY RESEARCH
Published by the
Iranian Chemical Society
www.physchemres.org
info@physchemres.org

Phys. Chem. Res., Vol. 11, No. 4, 929-942, December 2023
DOI: 10.22036/pcr.2023.356662.2170

Adsorption of Vanadium Using Amberlite IRA-68 Resin from Aqueous Solution: Kinetics and Thermodynamics Studies

D. Ghoddocy Nejad[a], A.R. Khanchi[a], M. Taghizadeh[b], H. Sid Kalal[a,*] and M. Outokesh[c]

[a]*Nuclear Fuel Research School, Nuclear Science and Technology Research Institute, AEOI, P. O. Box: 11365-3486, Tehran, Iran*
[b]*Chemical Engineering Department, Babol Noshirvani University of Technology, P. O. Box: 484, Babol 4714871167, Iran*
[c]*Department of Energy Engineering, Sharif University of Technology, Azadi Ave. Tehran, Iran*
(Received 17 August 2022, Accepted 3 January 2023)

The current study was aimed at elucidation of the adsorption properties of Amberlite IRA-68 resin for vanadium ions in aqueous media. We investigated the effect of different parameters such as contact time, pH, initial concentration, temperature, and adsorbent dosage on the uptake rate of vanadium. The findings showed that the equilibrium data were best fitted by the Freundlich isotherm, and the maximum adsorption capacity of the resin was 211.5 mg g^{-1} at 50 °C. The best possible pH for adsorption was 4.5. The first, and second-order reaction models and the Weber-Morris model were applied to the kinetics data. Among them, the best fitting was obtained by the second-order model. The rate-controlling step at the onset of the uptake was liquid film resistance, which gradually changed to intraparticle diffusion. Thermodynamic study revealed that adsorption was endothermic and spontaneous. The Amberlite IRA-68 resin could preserve more than 95% of its capacity after 8 cycles of adsorption/desorption.

Keywords: Vanadium adsorption, Amberlite IRA-68, Kinetics, Isotherm, Thermodynamic

INTRODUCTION

Vanadium is an important element for the steel industry that is added to alloys to increase strength. Other important uses of vanadium chemicals are as catalysts and pigments. Vanadium is a harmful heavy metal that occurs in industrial effluents, both in tetravalent and pentavalent forms, of which the pentavalent one is more hazardous [1]. Vanadium(V) is categorized as a dangerous environmental and occupational pollutant in the same class of toxicity as mercury, lead, and arsenic [2]. The element is present in significant concentration in fuel oil [3]; where according to some estimations, it is estimated to cause about 400,000 deaths from lung cancer, cardiovascular disease and about 14 million asthma diseases each year [1]. Different types of vanadium coexist in aqueous media. These are divided into three categories, cationic [*e.g.* VO_2^+], neutral [*e.g.* $VO(OH_3)$], and anionic species. The anionic group is also different. The speciation of vanadium in solutions is complex and highly dependent on its concentration and pH. Figure 1 shows the variation of these species with respect to pH [4-6]. To separate vanadium from aqueous solutions, so far, several methods have been investigated including chemical precipitation [7], membrane filtration [2], ion exchange [8,9], and adsorption [10,11]. In the case of the last two processes, the different types of adsorbents used to treat V(V)-containing wastewater were considered [8,10,11]. Adsorption effectiveness for vanadium removal depends mainly on the type of adsorbent (*i.e.* its functional groups) and pH of the solution [12-30]. For instance, Naeem et al. reported that on the adsorption of vanadium on different metal oxides, maximum uptake capacity is achieved between pH 3 to 4 [5]. Other researchers who employed coconut-derived active carbon, found the optimum pH between 4 and

*Corresponding author. E-mail: hsidkalal@aeoi.org.ir

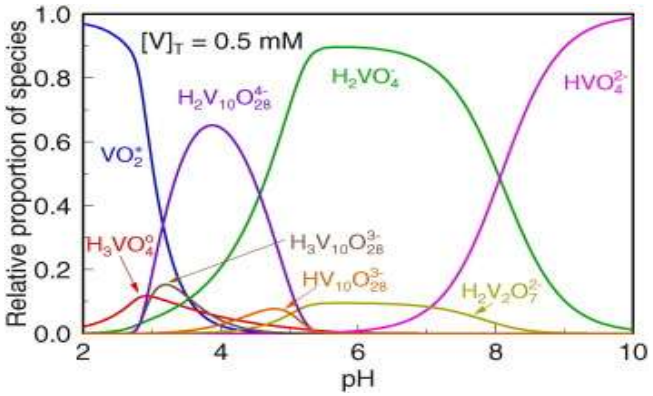

Fig. 1. Assignment of vanadium(V) species as a function of pH (C = 0.5 mM, T = 25 °C, 1 atm, ionic strength 0.15 M NaCl) taken from [32].

9 [31]. Studied the use of PGTFS (polyhydroxyethyl methacrylate-grafted tamarind skin)-$NH_3^+Cl^-$ for the adsorption of vanadium(V) ions, and they arrived at pHs 3 to 6 as the maximum capacity range. The aim of the current study was to investigate the efficiency of Amberlite IRA-68 anion exchange resin with a poly (hydroxyl ethylmethacrylate) structure and an $–NH_3^+Cl^-$ moiety, for the adsorption of vanadium(V) ions. The influence of different parameters such as pH, contact time, initial concentration, and adsorbent dosage on the uptake capacity of the resin was examined. Equilibrium, kinetic and thermodynamic studies were undertaken to elucidate different features of the adsorption process. Furthermore, the reusability of the IRA-68 resin was checked in eight consecutive cycles of adsorption-desorption.

EXPERIMENTAL

Materials and Instruments

The metal salts were analytical grade and were obtained from Merck, Germany. The stock solution of vanadium(V) (1000 mg l^{-1}) was prepared from sodium metavanadate by dissolving 2.23 g $NaVO_3$ in distilled water. Working solutions of various concentrations were obtained by diluting the stock solution with distilled water. due to the nature of weakly basic anion exchangers under different pH conditions. It has been observed that this type of anion exchanger shows a strong preference for heavy metal salts under neutral conditions and strong acids at low pH values. At neutral pH, the nitrogen atoms of these groups are not protonated. Therefore, they have a lone pair of electrons and can act as Lewis bases with metal ions (Lewis acids). In addition, equivalent amounts of anions must be present to maintain electroneutrality in the liquid phase and resin phase [33]. The physicochemical properties of Amberlite IRA-68 resin are as follows: Spherical beads of off-white to yellow color, ionic form with Cl, weakly basic amine, particle size 0.6-0.75 mm, and maximum service temperature 60 °C. The resin was prepared for the adsorption experiment by contacting it with a 5% (w/v) H2SO4 solution in the ratio 20:1 (V_{H2SO4}: M_{Resin}). The concentration of metal ions in solutions was determined using an inductively coupled plasma-optical atomic emission spectrometer (ICP-OES) (Perkin Elmer Optima 2000 DV, USA).

Experiments

The influence of pH on adsorption was determined by shaking 25 ml of vanadium solution with a fixed amount (0.1 g) of the adsorbent, for 4 h, in a thermostatic shaking bath. The rate of shaking was fixed at 200 strokes/min. The initial pH of the solutions was adjusted by adding adequate amounts of 0.5 M HNO_3 or 0.5 M NaOH solutions. After equilibration, samples were filtered using 0.45 µm nylon filter (Whatmann) and the concentration of vanadium ions was determined by (ICP-OES).

The adsorption rate, uptake capacity (q, mg g^{-1}), and distribution coefficient (K_d, ml g^{-1}) were calculated using the following equation:

$$Adsorption\ rate\,(\%) = \frac{(C_i - C_e)}{C_i} \times 100 \quad (1)$$

$$q(mg/g) = \frac{(C_i - C_e) \times V}{1000\,m} \quad (2)$$

$$K_d(ml/g) = \frac{(C_i - C_e)}{C_e} \times \frac{V}{m} \quad (3)$$

where C_i and C_e (mg l^{-1}) respectively denote the initial and equilibrium concentration of vanadium, V (ml) stands for volume of the solution, and m (g) shows the amount of adsorbent.

As for the evaluation of the adsorption capacity, two different procedures were undertaken. In the first procedure, the volume of the solution (25 ml), its initial concentration (70 mg l^{-1}) and temperature were set equal to the abovementioned values of the pH experiment, but the pH was 4.5 and the amount of the resin was changed from 0.5 to 10 g l^{-1}. In the second, initial concentration and amount of the resin were fixed, while the volume of the solution was changed.

Likewise, to study the kinetic of the vanadium uptake, we fixed the pH, temperature, and amount of the resin, but changed the initial concentration of vanadium. After the onset of the kinetic experiments, small amounts of solution were pipetted out at 5, 10, 15, 30, 60, 120, 180, and 240 min, and analyzed by ICP-OES method.

In order to estimate the thermodynamic parameters, uptake experiments were followed at different temperatures (30, 40, and 50 °C), with an initial vanadium concentration of 180 mg l^{-1}.

Another significant property, required for the industrial application, is reusability. This parameter in our study was evaluated by undertaking eight repeated cycles of adsorption-desorption, whereby the uptake percentage was measured at every cycle of the adsorption. In these experiments, desorption was performed by contacting the loaded resin with an adequately large amount of 2 M NaOH solution, followed by rinsing them with distilled water.

RESULTS AND DISCUSSION

Effect of pH

Figure 2 displays the effect of pH on the uptake efficiency of vanadium(V) by Amberlite IRA-68 resin. The adsorption percentage increased as pH rose from 2.0 to 4.5, and it reached a plateau in the range of pH 4.5-5.5. Afterwards, the uptake rate gradually decreased. At optimum pH ≈ 4.5, and initial V(V) concentrations of 70 and 150 mg l^{-1}, the amounts of adsorbed vanadium were found to be 49.6 and 79.8 mg g^{-1}, respectively.

The pH influences both ion speciation in the solution, and protonation/deprotonation in the resin matrix. As was explained in the introduction, vanadium exists in cationic forms below pH 3.0; and as VO_3^- ion in the pH range of 4.0-10.0 [4,6,34]. A decrease in the adsorption of vanadium in the pH range of 2.0 to 3.0. is indicative of positive vanadate

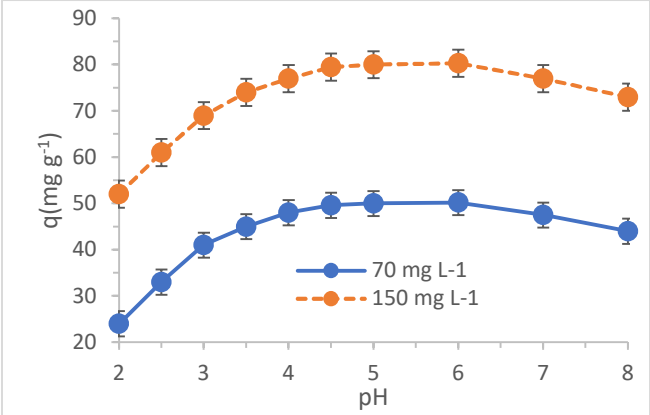

Fig. 2. Effect of pH on the uptake rate of Amberlite IRA-68 resin for V(V) ions (Temperature: 30 °C, Time: 4 h, Sorbent dose: 2 g l^{-1}).

species being repelled by protonated NH_2 groups of the ion exchanger. That maximum adsorption occurs at pH range of 4.0-5.0, indicates that anionic vanadium species predominates at such range, and it is preferentially adsorbed on amine groups of the resin. At higher pH values there is competition between hydroxide ions and anionic vanadium species for binding with amine groups.

Equilibrium Studies

Resin Dosages Effect. The relation between adsorbent dosage and uptake efficiency is shown in Fig. 3. According to this figure, by increasing adsorbent dosage, the uptake rate increases, but the loading of vanadium per unit mass of the adsorbent decreases. The increase in uptake percentage may be due to the increase in surface area and available adsorption sites, which are proportional to the amount of the resin [35]. On the other hand, the amount of adsorbent was changed from 0.5 to 10 g l^{-1}, which lowered the adsorption density from 95.4 to 5.1 mg g^{-1}, implying that an increase in the amount of adsorbent results in a higher density of unoccupied binding sites on Amberlite IRA-68 resin.

Adsorption capacity and isotherms. Figure 4 displays the equilibrium loading of the resin as a function of equilibrium concentration at three different temperatures of 30, 40, and 50 °C. The equilibrium distribution of solutes between the liquid and solid phases can best be described by the adsorption isotherms, for which various models such as *e.g.* B. Langmuir [36], Freundlich [37], Temkin [38], Radke-Prausnitz and Fritzschlunder [39] and compared the obtained

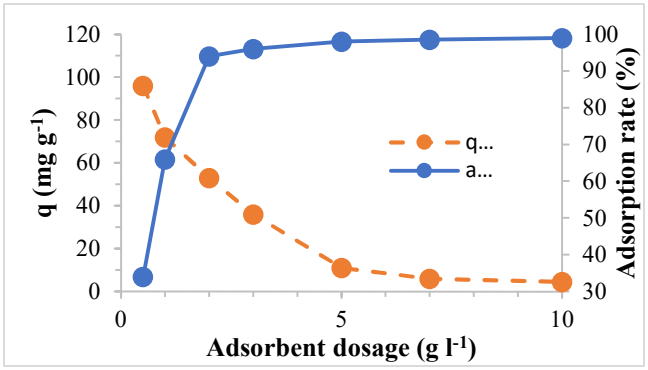

Fig. 3. Effect of adsorbent dosage on the adsorption of V(V) ions by Amberlite IRA-68 resin (Temperature: 30 °C, Time: 4 h, pH = 4.5, initial concentration: 150 mg l^{-1}).

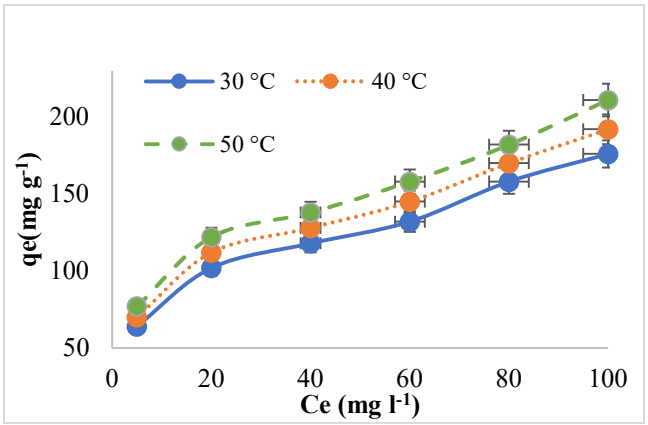

Fig. 4. Equilibrium uptake loading of vanadium on Amberlite IRA-68 resin at different temperatures (Time: 24 h, pH = 4.5, Sorbent dose: 2 g l^{-1}, initial concentration: 150 mg l^{-1}).

data with these generalized and nonlinear isotherm fitting curves studied for the above-mentioned adsorption isotherm models (Fig. 5).

The Langmuir model proposes monolayer adsorption with no mutual effects between the adsorbed species. This isotherm is expressed by:

$$q_e = \frac{Q_0 b C_e}{(1 + bC_e)} \quad (4)$$

where q_e (mg g^{-1}), and C_e (mg dm^{3-}) denote equilibrium values resin loading, and solution concentration, respectively. The constant Q_0 stands for maximum theoretical adsorption capacity, and b is related to the energy of adsorption.

The Freundlich isotherm model is expressed by:

$$q_e = K_f C_e^{\frac{1}{n}} \quad (5)$$

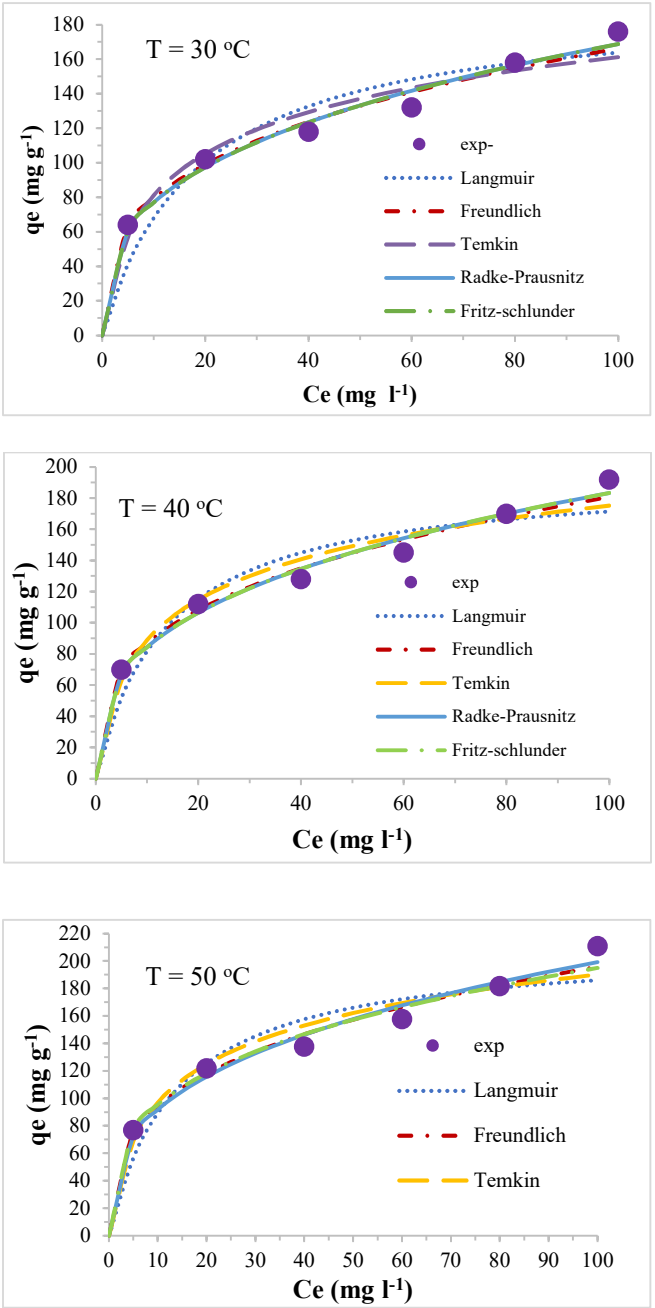

Fig. 5. Isotherm curves obtained by the best non-linear modeling at different temperatures for the removal of Vanadium ions on Amberlite IRA-68 resin (Time: 24 h, pH = 4.5, Sorbent dose: 2 g l^{-1}, initial concentration: 150 mg l^{-1}).

and in logarithmic form as:

$$\log q_e = \log K_f + \frac{1}{n} \log C_e \quad (6)$$

Table 1. Isotherm Constants of Different Models for Adsorption of Vanadium by Amberlite IRA-68

Isotherm	Parameter	T (°C)		
		30	40	50
Langmuir	q_{max}	194.2377	195.2	211.4729
	kI	0.054	0.07231	0.0733
	R^2	0.9581	0.8664	0.8517
	χ^2	12.79512	10.63851	12.51043
Freundlich	n	3.1072	3.1342	3.1747
	K_f (mg g^{-1}) (l mg^{-1})	37.7828	41.6018	45.9119
	R^2	0.9826	0.9827	0.9785
	χ^2	1.603808	1.692292	2.268974
Temkin	B (mg g^{-1})	34.7523	37.546	40.5294
	A (l mg^{-1})	1.0349	1.0662	1.0932
	R^2	0.9306	0.9319	0.9213
	χ^2	4.311822	4.47017	5.483634
Radke-Prausnitz	q_{max} (mg g^{-1})	7.324	8.244	9.016
	Krp (l mg^{-1})	99.98	99.93	99.94
	n	0.6593	0.6632	0.6639
	R^2	0.9736	0.9737	0.9667
	χ^2	1.661997	1.749802	2.358451
Fritz-schlunder	K1fs	44	41.88	46.76
	K2fs	0.2531	0.0786	0.0008
	n	0.3418	0.3372	0.3103
	m	0.004	0.000308	1.1E-07
	R^2	0.9737	0.9738	0.9623
	$\chi 2$	1.657203	1.746965	2.32486

where K_f is related to the adsorption capacity, and n indicates the selectivity. These constants were calculated from the nonlinear plot of q_e *vs*. C_0 (Fig. 5) and are presented in Table 1.

The Temkin isotherm is used in the forms of:

$$q_e = \frac{RT}{h} \ln(AC_e) \quad (7)$$

or:

$$q_e = B \ln A + B \ln C_e \quad (8)$$

where C_e and q_e have the equilibrium values, and RT/h = B and A and h are the constants. A plot of q_e *vs*. logC_e to check the applicability of Temkin model is given in Fig. 6.

Radke-Prausnitz isotherm. This model is particularly suitable for low adsorbate concentrations [40]. The isotherm is given by the following expression:

$$q_e = \frac{Q_{mRP}\ K_{RP} C_e}{(1+K_{RP} C_e)^{1/m_{RP}}} \quad (9)$$

Where qe is the adsorbed amount at equilibrium (mg g^{-1}), Q_{mRP} is the Radke-Prausnitz maximum adsorption capacities (mg g^{-1}), C_e is the adsorbate equilibrium concentration (mg l^{-1}), K_{RP} is the Radke-Prausnitz equilibrium constants and m_{RP} is the Radke-Prausnitz models exponents.

Fritz-Schlunder isotherm can be specified as follows:

$$q_e = \frac{K_{f1} C_e^{\ n_{fs}}}{1+K_{f2} C_e^{\ m_{fs}}} \quad (10)$$

qe (mg g^{-1}): equilibrium adsorption capacity, ce (mg l^{-1}): equilibrium adsorbate concentration in solution, k_{fl} (g^{-1}):

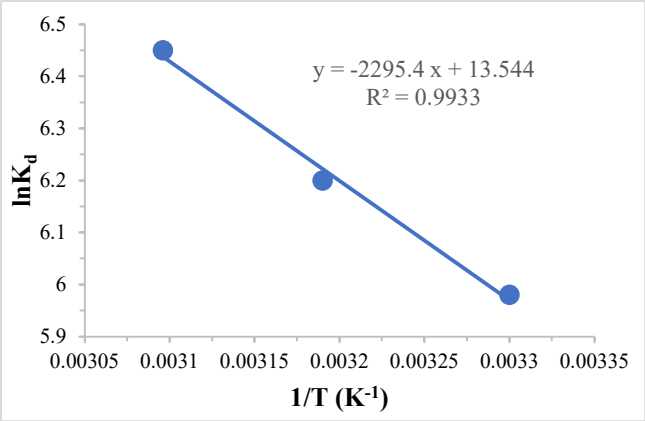

Fig. 6. Plot of $\ln K_d$ *vs.* 1/T for vanadium adsorption onto Amberlite IRA-68 resin. (Time: 4 h, pH = 4.5, Sorbent dose: 2 g l^{-1}, initial concentration: 150 mg l^{-1}).

Fritz-Schlunder constant, k_{f2} (mg^{-1}): Fritz-Schlunder constant, mf: Fritz-Schlunder exponent and nf: Fritz-Schlunder exponent.

According to Table 1, the adsorption of vanadium by Amberlite IRA-68 resin is of ion exchange nature. As shown in Table 1, The Freundlich model in the form of error Eqs. ((11) and (12)) as for R^2 and χ^2. The best fit among the isotherms used here. In addition, the values of the "n" parameter in the Freundlich model were greater than 1, showing the favorable nature of the uptake. The maximum adsorption capacity of Amberlite IRA-68 resin for vanadium was found to be 211.5 mg g^{-1}.

$$R^2 = 1 - \sum_{i=1}^{n} \frac{\left(x_{obs,i} - x_{model,i}\right)^2}{\left(x_{obs,i} - \overline{x_{model}}\right)^2} \quad (11)$$

$$\chi^2 = \sum_{i=1}^{n} \frac{\left(x_{obs,i} - x_{model,i}\right)^2}{x_{model,i}} \quad (12)$$

Comparison with other adsorbents. Table 2 shows comparisons of the adsorption capacities of various adsorbents with Amberlite IRA-68 resin for the uptake of vanadium ions. Evidently, Amberlite IRA-68 has an appreciable capacity for the V(V) uptake. Indeed, only Chitosan presents a higher capacity than the examined resin. But chitosan as a naturally modified biopolymer also has a remarkable capacity for ions such as copper or cadmium. Nonetheless, chitosan holds certain disadvantages compared to IRA-68 resin such as solubility in acidic media, and lesser durability, which restricts its large-scale application.

Thermodynamics of adsorption. Thermodynamics of adsorption was investigated to extend the applicability of the obtained data to wider range of the temperature. The required thermodynamic parameters were extracted from the data of distribution coefficient (K_d), which is defined as follows:

$$K_d\,(cm^3 g^{-1}) = \frac{C_i - C_e}{C_e} \times \frac{V}{m} \quad (13)$$

Table 2. Comparison of Adsorption Capacities of Various Adsorbents for Uptake of Vanadium

No.	Adsorbent	pH	Qmax (mg g^{-1})	Ref.
1	Activated carbon (Derived from starch industry waste sludge)	4.0	37.17	[40]
2	$ZnCl_2$-activated carbon	4-9	24.9	[31
3	Chitosan/a modified biopolymer	4.0	400	[12]
5	Iron-based adsorbent	3.0-4.0	111.11	[5]
6	Commercial spiral-wound	7.5	100	[2]
7	Zr(IV)-impregnated collagen fiber	5.0	96	[10]
8	Amberlite IRA-68 resin	4.5	211.5	This work

Standard free energy (ΔG^0), standard enthalpy (ΔH^0), and standard entropy (ΔS^0) were estimated by using the following equations [23]:

$$Ln(K_d) = \frac{\Delta S^0}{R} - \frac{\Delta H^0}{RT} \quad (14)$$

$$\Delta G^0 = \Delta H^0 - T\Delta S^0 \quad (15)$$

Where R is the universal gas constant.

Figure 6 shows a plot of the K_d *versus* the inverse of temperature. From the slope and intercept of the obtained line ΔH^0 and ΔS^0 can be calculated using Vant Hoff Eq. (14). The results are tabulated in Table 3.

Table 3. Thermodynamics Parameters for Vanadium Adsorption onto Amberlite IRA-68 Resin

Temperature (°C)	ΔG° (kJ mol^{-1})	ΔH° (kJ mol^{-1})	ΔS° (J mol K^{-1})
30	-15.03	19.08	112.57
40	-16.15	-	-
50	-17.28	-	-

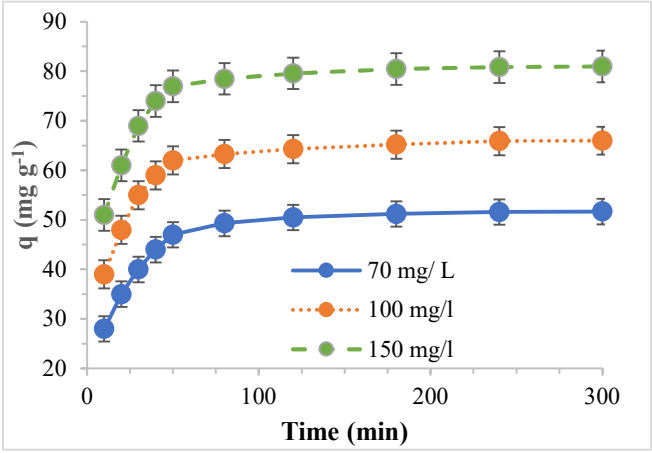

Fig. 7. Kinetics of V(V) uptake by Amberlite IRA-68 resin (Temperature: 30 °C, time: 4 h, Sorbent dose: 2 g l^{-1}, pH: 4.5)

Kinetic Studies

Figure 7 shows the effect of initial V(V) concentration and contact time on the adsorption rate of Amberlite IRA-68 resin. It can be seen that there was initially considerable adsorption (so 85%) for about 50 min and it levelled off, thereafter, to arrive at the equilibrium in nearly 4 h. Although change in the initial concentration of vanadium from 70 to 150 mg l^{-1}, led to a change in loading (q) from 47.3 to 77.6 mg g^{-1}, the equilibrium time was almost independent of the initial concentration. The relatively rapid initial uptake of V(V) ion is due to the adsorption of the ions on the surface of the adsorbent. According to Sag and Kutsal [41], the uptake of heavy metal ions often occurs in two successive stages: the first is rapid and quantitatively predominant, the second is slower and quantitatively insignificant. The slower stage can be related to the intraparticle transfer of the ions, whose diffusion coefficient is often smaller than the diffusivity of the ions in the liquid film medium. In addition, the initial rapid stage of the uptake is very likely due to the abundance of active sites of the resin at the onset of the adsorption [42]. The Sag and Kutsal theory encompasses the principal mass transfer resistances, but it overemphasizes on the share of the surface uptake in the rapid stage of adsorption and underestimates the contribution of intraparticle diffusion. Actually, the surface of the particle has only limited active sites, and most of the ion-sequestering sites are located in the interior body of the particle. At the onset of the adsorption, active sites of the surface are nearly promptly saturated by the exchanging ions. Afterward, the incoming ions have to penetrate into the volume of the resin through intraparticle diffusion, to be adsorbed. In the case of the Amberlite IRA-68 resin, high porosity enhances the intraparticle diffusion and augments the uptake kinetics. Generally speaking, faster kinetics is favored by the industry, because it corresponds to a smaller reactor size and a greater capital saving.

First-order and second-order kinetics. In order to acquire a deeper insight into the kinetics of uptake, and discover the rate-controlling mechanism of the adsorption, the experimental kinetic data were modeled using the first-order, the second-order, and the Weber-Morris equations. In what follows, we will first give a brief account of the aforementioned models and then go through their application on the obtained data.

Lagergren [43] suggested the first-order equation for the sorption of a solute, based on the solid capacity. His model is represented as:

$$\frac{dq}{dT} = k_1(q_e - q) \quad (16)$$

Where q_e and q denote loading of adsorbed ion (mg g^{-1}) on resin at the equilibrium and time t, respectively, and k_1 is the rate constant of the first-order adsorption (min^{-1}).

Integration of Eq. (16) with the initial conditions q = 0 at t = 0 gives:

$$Log(q_e - q) = Log(q_e) - k_1 t \quad (17)$$

`

The second-order kinetic model is represented by the following formula [44]:

$$\frac{dq}{dT} = k_2(q_e - q_t)^2 \quad (18)$$

Integration of Eq. (18) with the initial conditions q = 0 at t = 0 gives:

$$\frac{1}{q_e - q} = \frac{1}{q_e} + k_2 t \quad (19)$$

where k_2 (g mg min^{-1}) is the rate constant of the second-order adsorption. Slight manipulation of Eq. (19) results in the following formula that is more convenient for the depiction:

$$\frac{t}{q} = \frac{1}{k_2 q_e^2} + \frac{t}{q_e} \quad (20)$$

Figures 8 and 9 display the plot of kinetics data that were fitted to Eqs. (17) and (20). From the slope and intercepts of these graphs, the values of q_e and k_1 parameters of the first-

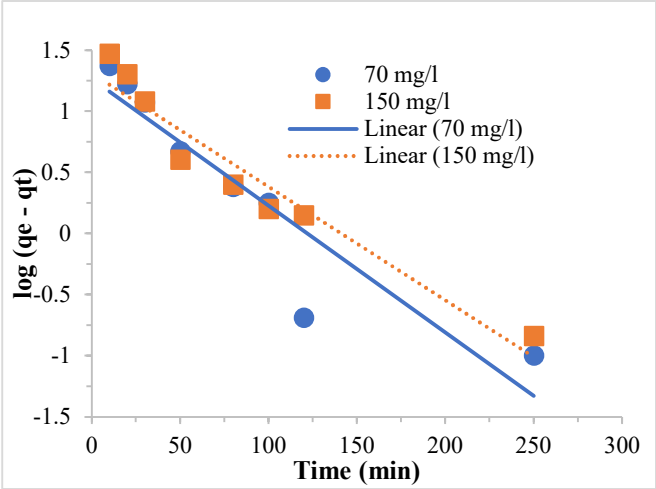

Fig. 8. Plots of the first-order kinetic model for adsorption of vanadium onto Amberlite IRA-68 resin (Temperature: 30 °C, pH: 4.5, adsorbent dose: 2 g l^{-1}).

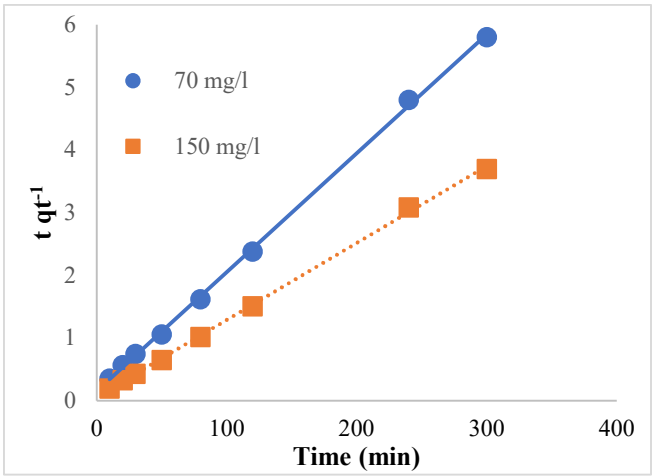

Fig. 9. Plots of the second-order kinetic model for adsorption of vanadium onto Amberlite IRA-68 resin (Temperature: 30 °C, pH: 4.5, adsorbent dose: 2 g l^{-1}).

Table 4. Values of Rate Constants for the First-order and Second-order Kinetic Models in Adsorption of Vanadium by AmberliteIRA-68 Resin, pH = 4.5, T = 30 °C, Resin = 2 g l^{-1}

C_i (mg l^{-1})	First order					Second order			
	K_1 (min^{-1})	$q_{e,exp}$ (mg g^{-1})	$q_{e,cal}$ (mg g^{-1})	R^2	SD	K_2 (g mg min^{-1})	$q_{e,cal}$ (mg g^{-1})	R^2	SD
70	0.035	51.3	26.5	0.932	0.065	0.0042	52.2	0.997	0.043
150	0.024	78.5	27.8	0.874	0.076	0.0018	79.6	0.999	0.033

order, and q_e and k_2 of the second-order models were obtained and tabulated in Table 4. Note that "q_e" somewhat acts as a fitting factor, and thus, its values differ in the different models.

According to Table 4, coefficients of determination (R^2) for the first-order kinetics are rather low, and the "q_e" values of this model do not agree well with the corresponding resin capacities, obtained from the equilibrium experiments. On the other hand, for the second-order model, R^2 values are close to unity, and calculated values of loading are close to their equilibrium counterparts. According to these results, the uptake kinetics of vanadium by Amberlite IRA-68, closely follows the second-order model [45]. We can conclude that the kinetics of the overall reaction depends on the concentrations of vanadate species and functional groups (amines) of the resin.

Weber-Morris model. There are three phenomena related to mass transport processes associated with the adsorption of ions from a solution. These are (1) film diffusion, (2) intraparticle or pore diffusion, and (3). The binding of adsorbate to the functional groups of ion exchangers. The third step has been found to be very rapid in ion exchange resins [46] and therefore, either intraparticle diffusion or film diffusion determines the overall adsorption rate.

In order to evaluate the main diffusion phenomena and kinetic data were also analyzed by Weber and Morris model [47]. For this purpose, the temporal loading of vanadium (q_t) was plotted against the square root of time using Eq. (21):

$$q_t = k_i t^{1/2} + C \qquad (21)$$

Where k_i (mg g^{-1} $min^{-0.5}$) is the intraparticle diffusion rate constant. The intercept C is an indication of the thickness of the liquid film layer, *i.e.*, the larger the intercept, the thinner the film layer, and the smaller the film mass transfer resistance [47,48].

The results of fitting the experiments with the Weber-Morris equation are shown in Fig. 10. Apparently, the uptake process comprises of two successive steps. According to Table 5, the first step has a higher k_i value, but a lesser C parameter. This means that at the beginning of the process, the liquid film resistance is larger and it controls the kinetics. With the progress of the adsorption, the near-surface layers of the resin are relatively quickly saturated, and ions have to diffuse through a longer length to reach the interior active sites of the resin. The consequence of this phenomenon is nothing but the enlargement of the intraparticle resistance. Such gradual change of the rate controlling mechanism is manifested by an increase in the C and a decrease in the k_i parameters.

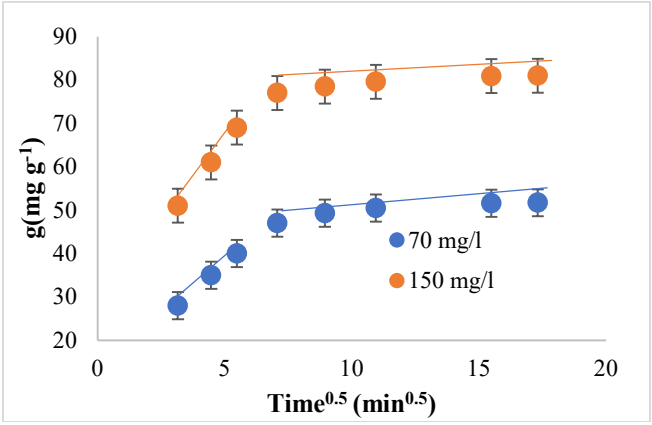

Fig. 10. Plots of the Weber and Morris kinetic model for adsorption of vanadium onto Amberlite IRA-68 resin (Temperature: 30 °C, pH: 4.5, Sorbent dose: 2 g l^{-1}).

Table 5. Values of the Weber-Morris Kinetic Constants for Uptake of Vanadium onto AmberliteIRA-68, pH = 4.5, T = 30 °C, Resin Dosage = 2 g l^{-1}

Ci (mg l^{-1})	Weber-Morris					
	$K_{i,1}$ (mg g^{-1} $min^{-0.5}$)	C_1	R_1^2	$K_{i,2}$ (mg g^{-1} $min^{-0.5}$)	C_2	R_2^2
70	5.18	11.69	0.99	0.41	45.08	0.84
150	7.75	26.45	0.99	0.37	74.93	0.92

An Overview of the reaction mechanism. As Fig. 1 shows, various species of negative vanadates involve in the adsorption of the resin. It is expected that these species almost transfer into the resin beads without any chemical changes under intraparticle diffusion. The previous studies showed that the reactions between vanadates and monoamine is weak, but their donor properties will improve when the number of alkyl groups on the amines increases. Under this condition, the stability of complexes grows by a factor of 2-3. In general, amine derivatives of amine react with various vanadate ions spontaneously and reversibly [49,50]. Our finding is also in agreement with these studies. For example, our results show that the ion exchange behavior of the resin with vanadate ions is reversible and they can be recovered from the resin with the change of pH condition. but here it appears that the overall reaction mechanism is not simple. *i.e.*, we can attribute a number of reactions to the resin which affects in the enthalpy of the overall reaction.

One of these reactions is that of vanadate deprotonation which is endothermic and occurs in dilute solutions (0.1 mM) as follows [51]:

$$H_2VO_4^- \rightleftharpoons \mathrm{H}VO_4^{2-} + H^+ \quad \Delta\mathrm{H} = 15 \pm 1\ \mathrm{KJ}\ mol^{-1} \qquad (22)$$

According to this model, oligomeric vanadates also can be converted to monomers under endothermic conditions, so that the exothermic interaction of amine groups and vanadate ions affects these reactions. In other words, the endothermic reaction of adsorption compensates by the increase of entropy because of increasing the number of free molecules in the solution with a concentration of 1mM considering the following equation [52]:

$$[\ M_xO_{4x-y}\ ]^{n-} + yH2O \ \rightleftharpoons\ \mathrm{x}MO_4^{a-} + 2\mathrm{y}H^+ \qquad (23)$$

In addition to the above, we can assign the role of ion pair interaction in this adsorption mechanism. Accordingly, the binding of monomeric vanadates with amine groups is stronger than oligomeric ones. *i.e.*, charge density is higher in small species than oligomers. In other words, the monomeric solvent-separated ion pair species will form conveniently when these anions compete against oligomeric vanadate.

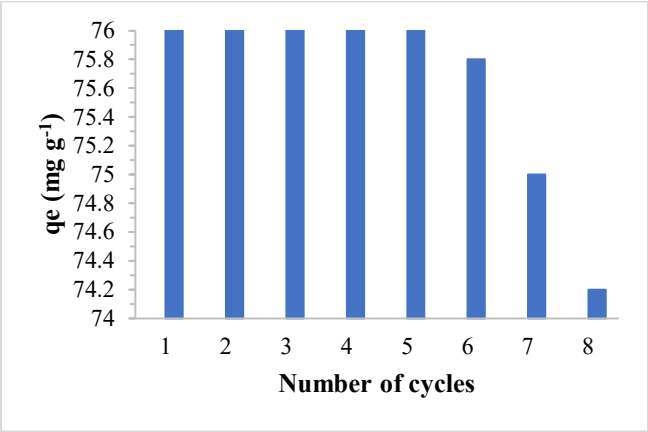

Fig. 11. Effect of regeneration cycle on adsorption capacity of Amberlite IRA-68 resin for V(V) ions (initial concentration:150 mg l^{-1}, solution pH = 4.5, mass of adsorbent 2 g l^{-1} and T = 30 °C).

Desorption and Reusability

In order to study the durability and reusability of the adsorbent, multiple cycles of adsorption-desorption were conducted on the same resin substance. After each cycle, an alkaline solution (2 M NaOH) was employed as the stripping agent and a double distilled water as the washing liquid. The obtained results are shown in Fig. 11. According to this figure, the uptake capacity of Amberlite IRA-68 resin decreased by about 5% after eight cycles of adsorption-desorption. Such reduction is rather insignificant and can be resulted from incomplete elution of vanadium between the cycles. As a result, Amberlite IRA-68 seems to have noticeable stability and reusability in the uptake of vanadium.

CONCLUSIONS

The current study demonstrated that Amberlite IRA-68 is an effective adsorbent of vanadium in the aqueous media. Thermodynamic study revealed that the adsorption of vanadium onto Amberlite IRA-68 is spontaneous, and its extent of progress is improved by increasing the temperature (*i.e.* it is endothermic). The adsorption capacity was found to be 211.5 mg g^{-1}, which is quite appreciable for an anion exchange resin. Among the adsorption isotherms, the Freundlich equation best fitted the equilibrium data. The uptake percentage was largely dependent on pH, and the

optimum pH was found to be around 4.5. Adsorption of V(V) by Amberlite IRA-68 resin was quite rapid in the first 50 min, and it attained equilibrium in 250 min. The adsorption rate followed a second-order kinetic model very closely. The positive value of ΔH^0 indicates an endothermic process with regard to the adsorption of vanadium. The negative free energy change, the positive entropy change, the adsorption process is spontaneous and favors the higher temperatures. Also fitting the kinetics data with the Weber-Morris mechanistic model revealed that the rate-controlling mechanism at the onset of adsorption was liquid film resistance, which gradually changed to intraparticle diffusion. Amberlite IRA-68 resin can be reused for the adsorption of vanadium for at least eight cycles without significant loss of the uptake capacity. In summary, Amberlite IRA-68 anion exchange resin is an excellent adsorbent for the large-scale recovery of anionic vanadium complexes in industry.

ACKNOWLEDGEMENTS

The authors would like to acknowledge all those who aided in this work and the nuclear science and technology research institute in Tehran for financial and technical support.

REFERENCES

[1] Patel, B.; Henderson, G. E.; Haswell, S. J.; Grzeskowiak, R., Speciation of vanadium present in a model yeast system. *Analyst*. **1990**, *115*, 1063-1066, DOI: 10.1039/an9901501063.

[2] Lazaridis, N. K.; Jekel, M.; Zouboulis, A. I., Removal of Cr(VI), Mo and V(V) ions from single metal aqueous solutions by sorption or nanofiltration. *Sep. Sci. Technol*. **2003**, *38* (10), 2201-2219, DOI: 10.1081/SS-120021620.

[3] Guzman, J.; Saucedo, I.; Navaro, R.; Revilla, J.; Guibal, E., Vanadium interactions with chitosan: influence of polymer protonation and metal speciation. *Lungmuir.* **2002**, *18*, 1567-1573, DOI: 10.1021/la010802n

[4] Bao, S.; Duan, J.; Zhang, Y., Recovery of V(V) from complex vanadium solution using capacitive deionization (CDI) with resin/carbon composite electrode. *Chemosphere* **2018**, *208*, 14-20, DOI: 10.1016/j.chemosphere.2018.05.149.

[5] Xiaobo, Z.; Wang, L.; Sen, T.; Majian, Z.; Pengyuan, B.; Lunjian, C., Selective recovery of vanadium and scandium by ion exchange with D201 and solvent extraction using P507 from hydrochloric acid leaching solution of red mud. *Chemosphere.* **2017**, *175*, 365-372, DOI: 10.1016/j.chemosphere.2017.02.083.

[6] Peacock, C. L.; Sherman, D. M., Vanadium(V) adsorption onto goethite at ph 1.5 to 12: a surface complexation model based on ab initio molecular geometries and EXAFS spectroscopy, Geochim. *Cosmochin. Acta*. **2004**, 68, 1723-1733, DOI: 10.1016/j.gca.2003.10.018. 52.

[7] Peng, H.; Liu, Z.; Tao, C., Adsorption Process of Vanadium(V) with Melamine. *Water, Air, Soil Pollut.* **2017**, 228, 272, DOI: 10.1007/s11270-017-3452-z

[8] Yeom, B. Y.; Lee, C. S.; Hwang, T. S., A new hybrid ion exchanger: effect of system parameters on the adsorption of vanadium(V). *J. Hazard. Mater.* **2009**, 166, 415-420, DOI: 10.1016/j.jhazmat.2009.03.137.

[9] Zhu, X.; Li, W.; Zhang, C.; Chen, I., Separation characteristics of vanadium from leach liquor of red mid by ion exchange with different resins. *Hydrometallurgy*. **2018**, 176, 42-48, DOI: 10.1016/j.hydromet.2018.01.009.

[10] Kavakli, P. A.; Seko, N.; Tamada, M.; Guven, O., Adsorption efficiency of a new adsorbent towards uranium and vanadium ions at low concentrations. *Sep. Sci. Techn.* **2005**, *39* (7), 1631-1643, DOI: 10.1007/S40995-021-01156.

[11] Liao, X. P.; Tang, W.; Zhou, R. Q.; Shi, B., Adsorption of metal anions of vanadium(V) and chromium(VI) on Zr(IV) impregnated collagen fiber, *Adsorption*. **2008**, *14* (1), 55-64, DOI: 10.1007/s10450-007-9045-1.

[12] Hao, L.; He, Y.; Shi, C.; Hao, X., Biologically removing vanadium(V) from groundwater by agricultural biomass. *J. Environ. Manag*. **2021**, *296*, 113244, DOI: 10.1016/j.jenvman.2021.113244.

[13] Peng, H.; Liu, Z.; Tao, C., Adsorption kinetics and isotherm of vanadium with melamine. *Water Sci. Technol.* **2017**, *75*, 2316-2321, DOI: 10.2166/wst.2017.094.

[14] He, W.; Liao, W.; Yang, J.; Jeyakumar, P.; Anderson,

C., Removal of vanadium from aquatic environment using phosphoric acid modified rice straw. *Ann. Finance*. **2020**, *24*, 80-89, DOI: 10.1080/10889868.2020.1724073.

[15] Jiang, Y.; Yin, X.; Luo, X.; Yu, L.; Sun, H.; Wang, N.; Mathews, S., Sorption of vanadium(V) on three typical agricultural soil of the Loess Plateau, *China. Environ. Pollut. Bioavailab*. **2019**, *31*, 120-130, DOI: 10.1080/26395940.2019.1590162.

[16] Kajjumba, G. W.; Aydın, S.; Güneysu, S., Adsorption isotherms and kinetics of vanadium by shale and coal waste. *Adsorpt. Sci. Technol*. **2018**, *36*, 936-952, DOI: 10.1177/026361741773358.

[17] Liu, X.; Zhang, L., Insight into the adsorption mechanisms of vanadium(V) on a high-efficiency biosorbent (Ti-doped chitosan bead). *Int. J. Biol. Macromol*. **2015**, *79*, 110-117, DOI: 10.1016/j.ijbiomac.2015.04.065.

[18] Liu, Z.; Zhang, Y.; Dai, Z.; Huang, J.; Liu, C., Coextraction of vanadium and manganese from high-manganese containing vanadium wastewater by a solvent extraction-precipitation process. *Front. Chem. Sci. Eng*. **2020**, *14*, 902-912. DOI: 10.1007/s11705-019-1887-z.

[19] Meng, R.; Chen, T.; Zhang, Y.; Lu, W.; Liu, Y.; Lu, T.; Liu, Y.; Wang, H., Development, modification, and application of low-cost and available biochar derived from corn straw for the removal of vanadium(V) from aqueous solution and real contaminated groundwater. *RSC Adv*. **2018**, *8*, 21480-21494, DOI: 10.1039/c8ra02172d.

[20] Omidinasab, M.; Rahbar, N.; Ahmadi, M.; Kakavandi, B.; Ghanbari, F.; Kyzas, G. Z.; Martinez, S. S.; Jaafarzadeh, N., Removal of vanadium and palladium ions by adsorption onto magnetic chitosan nanoparticles. *Environ. Sci. Pollut. Res*. **2018**, *25*, 34262-34276, DOI: 10.1007/s11356-018-3137-1.

[21] Polowczyk, I.; Cyganowski, P.; Urbano, B. F.; Rivas, B. L.; Bryjak, M.; Kabay, N., Amberlite IRA-400 and IRA-743 Chelating Resins for the Sorption and Recovery of molybdenum(VI) and vanadium(V): Equilibrium and Kinetic Studies. *Hydrometallurgy*. **2017**, 169, 496-507, DOI: 10.1016/j.hydromet.2017.02.017.

[22] Salehi, S.; Anbia, M., Performance comparison of chitosan-clinoptilolite nanocomposites as adsorbents for vanadium in aqueous media. *Cellulose*. **2019**, *26*, 5321-5345, DOI: 10.1007/s10570-019-02450-9.

[23] Yu, Y.; Wei, Q.; Li, J.; Yang, J., Removal of vanadium from wastewater by multi-walled carbon nanotubes. *Fullerenes Nanotub. Carbon Nanostructures*. **2017**, *25*, 170-178, DOI: 10.1080/1536383X.2016.1274306.

[24] Zhu, H.; Xiao, X.; Guo, Z.; Han, X.; Liang, Y.; Zhang, Y.; Zhou, C., Adsorption of vanadium(V) on natural kaolinite and montmorillonite: characteristics and mechanism. *Appl. Clay Sci*. **2018**, *161*, 310-316, DOI: 10.1016/j.clay.2018.04.035.

[25] Zhu, H.; Xiao, X.; Guo, Z.; Peng, C.; Wang, X.; Yang, A., Characteristics and behaviour of vanadium(V) adsorption on goethite and birnessite. *Environ. Earth Sci.* **2020**, *79*, 1-10, DOI:10.1007/s12665-020-08992-7.

[26] Wadhwa, S. K.; Tuzen, M.; Gul Kazi, T.; Soylak, M., Graphite furnace atomic absorption spectrometric detection of vanadium in water and food samples after solid phase extraction on multiwalled carbon nanotubes. *Talanta,* **2013**, *116*, 205-209, DOI: org/10.1016/j.talanta.2013.05.020.

[27] Naeemullah, A.; Tuzen, M.; Gul Kazi, T.; Citak, D.; Soylak, M., Pressure-assisted ionic liquid dispersive microextraction of vanadium coupled with electrothermal atomic absorption spectrometry. *J. Anal. At. Spectrom*., **2013**, *28*, 1441-1445, DOI: 10.1039/c3ja50174d.

[28] Saleh, T. A.; Elsharif, A. M.; Bin-Dahman, O. A., Synthesis of amine functionalization carbon nanotube-low symmetry porphyrin derivatives conjugates toward dye and metal ions removal. *J. Mol. Liq*. **2021**, *340*, 117024, DOI: 10.1016/j.mollig.2021.117024.

[29] Saleh, T. A.; Mustaqeem, M.; Khaled, M., Water treatment technologies in removing heavy metal ions from wastewater: A review. *Environ. Nanotechnol. Monit. Manag.* **2022**, *17*, 100617, DOI: 10.1016/j.enmm.2021.100617.

[30] Saleh, T. A., Protocols for synthesis of nanomaterials, polymers, and green materials as adsorbents for water treatment technologies. *Environ. Technol. Innov*., **2021**, *24*, 101821, DOI: 10.1016/j.eti.2020.101821.

[31] Namasivayam, C.; Sangeetha, D., Removal and recovery of vanadium(V) by adsorption onto $ZnCl_2$ activated carbon: kinetic and isotherms. *Adsorption*, **2006**, *12* (2), 103-117. DOI: 10.1007/s10450-006-0373-3.

[32] Kurniawan, T. A.; Chan, G. Y. S.; Lo, W. H.; Babel, S. Physicochemical treatment techniques for wastewater laden with heavy metals. *Chem. Eng. J.* **2006**, 118, 83-89. DOI: 10.1016/j.cej.2006.01.015.

[33] Huang, J.H.; Huang, F.; Evans, L.; Glasauer, S., Vanadium: Global (bio) geochemistry. *Chem. Geol.* **2015**, 417, 68-89. DOI: 10.1016/ j.chemgeo.2015.09.019.

[34] Peng, H.; Shang, Q.; Chen, R.; Zhang, L.; Chen, Y.; Guo, J., Step-Adsorption of Vanadium(V) and Chromium(VI) in the Leaching Solution with Melamine. *Sci Rep.* **2020**, *10*, 6326, DOI: 10.1038/ s41598-020-63359-z.

[35] Fan, F. L.; Qin, Z.; Bai, J.; Rong, W. D.; Fan, F. Y.; Tian, W.; Zhao, l., Rapid removal of uranium from aqueous solutions using magnetic Fe_3O_4 SiO_2 composite particles. *J. Environ. Radioact.* **2012**, *106*, 40-46, DOI: 10.1016/j.jenvrad.2011.11.003.

[36] Langmuir, I., The adsorption of gases on plane surface of glass, mica and platinum. *J. Am. Chem. Soc.* **1918**, *40* (9),1361-1403, DOI: 10.1021/ja02242a004.

[37] Peng, H.; Wang, F.; Li, G.; Guo, J.; Li, B., Highly Efficient Recovery of Vanadium and Chromium: Optimized by Response Surface Methodology. *ACS Omega.* **2019**, *4*, 904-910, DOI: 10.1021/ acsomega.8b02708.

[38] Wu, C. H., Adsorption of reactive dye onto carbon nanotubes: Equilibrium, kinetics and thermodynamics. *J. Hazard. Mater.* **2007**, *144*, 93-100, DOI: 10.1016/ j.jhazmat.2006.09.083.

[39] Syafiuddin, A.; Salmiati, S.; Jonbi, J.; Fulazzaky, M. A., Application of the kinetic and isotherm models for better understanding of the behaviors of silver nanoparticles adsorption onto different adsorbents, *J. of Env. Manag*. **2018**, *218*, 59-70, DOI: 10.1016/ j.jenvman.2018.03.066.

[40] Afroze, S.; Sen, T. K.; Ang, M.; Nishioka, H., Adsorption of methylene blue dye from aqueous solution by novel biomass Eucalyptus sheathiana bark: equilibrium, kinetics, thermodynamics and mechanism. *Desalin. Water Treat.* **2016**, *57*, 5858-5878, DOI: 10.1080/19443994.2015.1004115.

[41] Ozcan, A. S.; Erdem, B.; Ozcan, A., Adsorption of Acid blue 913 from Aqueous Solutions onto BTMA-bentonite*, Colloids Surf. A Physicochem.* **2005**, *266*, 73-81, DOI: 10.1016/j.jcis.2004.07.035.

[42] Sari, A.; Tuzen, M.; Citak, D.; Soylak, M., Adsorption characteristics of Cu(II) and Pb(II) onto expanded perlite from aqueous solution, *J. Hazard Mater*. **2007**, *148* (1-2), 387-394, DOI: 10.1016/ j.jhazmat.2007.02.052.

[43] Konggidinata, M. I.; Chao, B.; Lian, Q.; Subramaniam, R.; Zappi, M.; Gang, D. D., Equilibrium, kinetic and thermodynamic studies for adsorption of BTEX onto Ordered Mesoporous Carbon (OMC). *J. Hazard. Mater.* **2017**, *336*, 249-259, DOI: 10.1016/ j.jhazmat.2017.04.073.

[44] Tangtubtim, S.; Saikrasun, S., Adsorption behavior of polyethyleneimine-carbamate linked pineapple leaf fiber for Cr(VI) removal. *Appl. Surf. Sci.* **2019**, *467-468*, 596-607, DOI: 10.1016/j.apsusc.2018.10.204.

[45] Ho, Y. S.; McKay, G., Pseudo-second order model for sorption processes. *Process Biochem.* **1999**, *34*, 451-465, DOI: 10.1016/S0032-9592(98)00112-5.

[46] Dogan, V.; Aydin, S., vanadium(V) removal by adsorption onto activated carbon derived from industry waste sludge. *Sep. Sci. Technol.* **2014**, *49*, 1407-1415, DOI: 10.1080/01496395.2013.879312.

[47] Weber Jr, W. J.; Morris, J. C., Kinetics of adsorption on carbon from solution, *J. Sanit. Eng. Div. ASCE* **1963**, *89* (2), 31-60, DOI: 10.1061/JSEDAI.0000430.

[48] Mall, I. D.; Srivastava, V. C.; Agarwal, N. K., Removal of Orange-G and Methyl Violet dyes by adsorption onto bagasse fly ash-kinetic study and equilibrium isotherm analyses, *Dyes Pig*. **2006**, *69*, 210-223, DOI: 10.4236/ jwarp.2013.57A003.

[49] Crans, D. C.; Ehde, P. M.; Shin, P. K.; Pettersson, L., Spontaneous and reversible interaction of vanadium(V) oxyanions with amine derivatives, *Inorg. Chem.* **1988**, 1797-1806, DOI: 10.1021/ic00283a025.

[50] Alan, S.; Tracey, G. R.; Willsky, E.; Takeuchi, S., *Vanadium: chemistry, biochemistry, pharmacology, and practical applications*, **2007**, CRC Press, p. 33-34.

[51] McCann, N.; Wagner, M.; Hasse, H., A thermodynamic model for vanadate in aqueous solution-equilibria and reaction enthalpies, *Dalton Trans*. **2013**, *42*, 2622-2628, DOI: 10.1039/c2dt31993d.

[52] Müller, W. E. G.; Wang, X.; Schröder, H. C., *Biomedical Inorganic Polymers: Bioactivity and Applications of Natural and Synthetic Polymeric Inorganic Molecules, in Progress in Molecular and Subcellular Biology,* **2013**, Springer, p. 12-14.